

## Coupled-Channel Evaluations of Cross Sections for Scattering Involving Particle-Unstable Resonances

P. Fraser,<sup>1,\*</sup> K. Amos,<sup>1</sup> L. Canton,<sup>2</sup> G. Pisent,<sup>2</sup> S. Karataglidis,<sup>3</sup> J. P. Svenne,<sup>4</sup> and D. van der Knijff<sup>5</sup>

<sup>1</sup>*School of Physics, University of Melbourne, Victoria 3010, Australia*

<sup>2</sup>*Istituto Nazionale di Fisica Nucleare, Sezione di Padova, I-35131, Italy*

<sup>3</sup>*Department of Physics and Electronics, Rhodes University, Grahamstown 6140, South Africa*

<sup>4</sup>*Department of Physics and Astronomy, University of Manitoba, Winnipeg, Manitoba, Canada R3T 2N2*

<sup>5</sup>*Advanced Research Computing, Information Division, University of Melbourne, Victoria 3010, Australia*

(Received 27 June 2008; published 12 December 2008)

How does the scattering cross section change when the colliding bound-state fragments are allowed particle-emitting resonances? This question is explored in the framework of a multichannel algebraic scattering method of determining nucleon-nucleus cross sections at low energies. Two cases are examined, the first being a gedanken investigation in which  $n + {}^{12}\text{C}$  scattering is studied with the target states assigned artificial widths. The second is a study of neutron scattering from  ${}^8\text{Be}$ , a nucleus that is particle unstable. Resonance character of the target states markedly varies evaluated cross sections from those obtained assuming stability in the target spectrum.

DOI: 10.1103/PhysRevLett.101.242501

PACS numbers: 24.10.Eq, 24.30.-v, 25.40.-h, 25.60.-t

The advent of radioactive ion beam physics poses new theoretical challenges involving weakly bound systems. For instance, coupled-channel analyses so far assumed nuclei to have spectra of zero-width states. Radioactive nuclei, and especially those near the drip lines, can have quite low particle emission thresholds and thus low-lying resonance states in their spectra. This Letter considers how that characteristic can influence properties of scattering and the compound spectrum. The ready availability of radioactive ion beam allows experimental information to be obtained on many exotic nuclei, allowing study of novel structures, such as skins and halos. Of particular interest is data obtained from scattering exotic nuclei from hydrogen targets, which equates to proton scattering from those nuclei in the inverse kinematics. Such data have been analyzed in terms of effective nucleon-nucleus interactions used in distorted wave approximations [1–3], or by coupled-channels approaches [4,5].

This Letter considers low-energy neutron scattering from light mass nuclei for which discrete resonance effects in the elastic cross section are usually present. Such resonance properties most often result from channel coupling and are reproduced here using a multichannel algebraic scattering (MCAS) theory [5]. With MCAS, solutions of coupled Lippmann-Schwinger equations are found (in momentum space) by using finite-rank separable representations of an input matrix of nucleon-nucleus interactions. An “optimal” set of sturmian functions [6] is used as the expansion set. Details are given in Refs. [5,7].

Advantages of using the MCAS method include an ability to locate all compound system resonance centroids and widths regardless of how narrow they may be, and, by use of orthogonalizing pseudopotentials in generating sturmians, to ensure the Pauli principle is not violated [7],

despite the collective model formulation of nucleon-nucleus interactions used therein. The latter is of paramount importance for coupled-channel calculations [8], as otherwise some compound nucleus wave functions so defined possess spurious components.

MCAS is used to find solutions of the coupled-channel, partial-wave expanded Lippmann-Schwinger equations for each total system spin-parity ( $J^\pi$ ),

$$T_{cc'}^{J\pi}(p, q; E) = V_{cc'}^{J\pi}(p, q) + \mu \left[ \sum_{c''=1}^{\text{open}} \int_0^\infty V_{cc''}^{J\pi}(p, x) \times \frac{x^2}{k_{c''}^2 - x^2 + i\epsilon} T_{c''c'}^{J\pi}(x, q; E) dx - \sum_{c''=1}^{\text{closed}} \int_0^\infty V_{cc''}^{J\pi}(p, x) \times \frac{x^2}{h_{c''}^2 + x^2} T_{c''c'}^{J\pi}(x, q; E) dx \right], \quad (1)$$

where a finite set of scattering channels, denoted  $c$ , is considered, and where  $\mu = \frac{2\bar{m}}{\hbar}$ ,  $\bar{m}$  being the reduced mass. There are two summations as the open and closed channel components are separated, with wave numbers

$$k_c = \sqrt{\mu(E - \epsilon_c)} \quad \text{and} \quad h_c = \sqrt{\mu(\epsilon_c - E)}, \quad (2)$$

for  $E > \epsilon_c$  and  $E < \epsilon_c$ , respectively.  $\epsilon_c$  is the energy threshold at which channel  $c$  opens (the excitation energies of the target nucleus). Henceforth the  $J^\pi$  superscript is to be understood. Expansion of  $V_{cc'}$  in terms of a finite number ( $N$ ) of sturmians leads to a separable representation of the scattering matrix [5]

$$S_{cc'} = \delta_{cc'} - i^{(l_{c'} - l_c + 1)} \pi \mu \sum_{n,n'=1}^N \sqrt{k_c} \hat{\chi}_{cn}(k_c) [\boldsymbol{\eta} - \mathbf{G}_0]^{-1} \hat{\chi}_{c'n'}(k_{c'}) \sqrt{k_{c'}}. \quad (3)$$

$c$  and  $c'$  refer now only to open channels,  $l_c$  is the partial wave in channel  $c$ , and the Green function matrix is

$$[\mathbf{G}_0]_{nn'} = \mu \left[ \sum_{c=1}^{\text{open}} \int_0^\infty \hat{\chi}_{cn}(x) \frac{x^2}{k_c^2 - x^2} \hat{\chi}_{c'n'}(x) dx - \sum_{c=1}^{\text{closed}} \int_0^\infty \hat{\chi}_{cn}(x) \frac{x^2}{h_c^2 + x^2} \hat{\chi}_{c'n'}(x) dx \right]. \quad (4)$$

$\boldsymbol{\eta}$  is a column vector of sturmian eigenvalues and  $\hat{\chi}$  are form factors determined from the chosen sturmian functions. Details are given in Ref. [5].

Traditionally, all target states are taken to have eigenvalues of zero width and the (complex) Green functions are evaluated using the method of principal parts. This assumes time evolution of target states is given by

$$|x, t\rangle = e^{-iH_0 t/\hbar} |x, t_0\rangle = e^{-iE_0 t/\hbar} |x, t_0\rangle. \quad (5)$$

However, if states decay, they evolve as

$$|x, t\rangle = e^{-(\Gamma/2)t} e^{-iE_0 t/\hbar} |x, t_0\rangle. \quad (6)$$

Thus, in the Green function, channel energies become complex, as do the squared channel wave numbers,

$$\hat{k}_c^2 = \mu \left( E - \epsilon_c + \frac{i\Gamma_c}{2} \right); \quad \hat{h}_c^2 = \mu \left( \epsilon_c - E - \frac{i\Gamma_c}{2} \right), \quad (7)$$

where  $\frac{\Gamma_c}{2}$  is half the width of the target state associated with channel  $c$ . The Green function matrix elements then are

$$[\mathbf{G}_0]_{nn'} = \mu \left[ \sum_{c=1}^{\text{open}} \int_0^\infty \hat{\chi}_{cn}(x) \times \frac{x^2}{k_c^2 - x^2 + (i\mu\Gamma_c/2)} \hat{\chi}_{c'n'}(x) dx - \sum_{c=1}^{\text{closed}} \int_0^\infty \hat{\chi}_{cn}(x) \times \frac{x^2}{h_c^2 + x^2 - (i\mu\Gamma_c/2)} \hat{\chi}_{c'n'}(x) dx \right], \quad (8)$$

where  $k_c$  and  $h_c$  are as in Eq. (2). With poles moved significantly off the real axis, integration of a complex integrand along the real momentum axis is feasible. This has been done. However, for any infinitesimal-width target state, or resonance so narrow that it can be treated as such, the method of principal parts has been retained. To illustrate we consider two cases of low-energy neutron scattering: from  $^{12}\text{C}$  and from  $^8\text{Be}$ .

As done previously [5,7], the  $^{13}\text{C}$  ( $n + ^{12}\text{C}$ ) system is studied using the MCAS approach with a rotational model

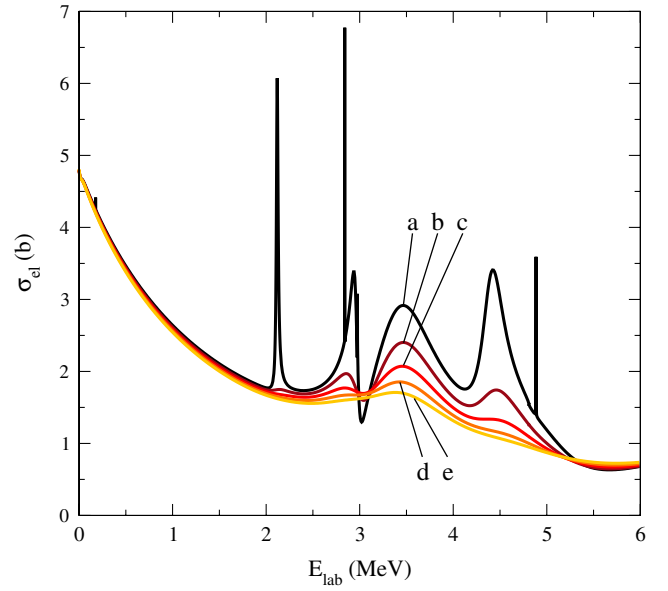


FIG. 1 (color online). Calculated cross sections for hypothetically  $n$ -(unstable)  $^{12}\text{C}$  scattering as functions of neutron energy. Labels as per Table I.

prescription of the matrix of interaction potentials connecting three states of  $^{12}\text{C}$  [the  $0_{\text{g.s.}}^+$ ,  $2_1^+$  (4.43 MeV) and  $0_2^+$  (7.64 MeV)]. The same interaction Hamiltonian has been used and allowance made for Pauli blocking via the orthogonalizing pseudopotentials scheme. In the first instance, all three states are considered zero width, giving the elastic scattering cross section of neutrons to 6 MeV as previously published. Additionally, evaluations are made for the same interaction allowing the  $2_1^+$  and  $0_2^+$  states of  $^{12}\text{C}$  to have particle emission widths of varying size; the ground state kept with zero width. Results are displayed in Fig. 1.

Cross sections follow a marked trend as hypothetical state widths increase. Widths used are listed in Table I. Ascribing the first widths to the excited states [set (b)], very narrow resonances in the original cross section disappear. In the earlier studies [5,7], it is noted that those (narrow) compound resonance states are dominated by the coupling of an  $sd$ -shell nucleon to the  $2_1^+$  state in  $^{12}\text{C}$ . The broader resonances remain evident in the cross section as the state widths are artificially increased. However, with these increases, the remaining resonances smear out. In the case of the broadest target states [set (e)] the cross section

TABLE I. Artificial widths ( $\Gamma$ , in MeV) assigned to  $^{12}\text{C}$  states.

Curve	$0_1^+$ width	$2_1^+$ width	$0_2^+$ width
a	0.00	0.00	0.00
b	0.00	0.20	0.60
c	0.00	0.40	1.20
d	0.00	0.60	1.80
e	0.00	0.80	2.40

TABLE II. Widths (in MeV) for  $^{13}\text{C}$  states from calculation allowing states of  $^{12}\text{C}$  to be resonances as listed in Table I.

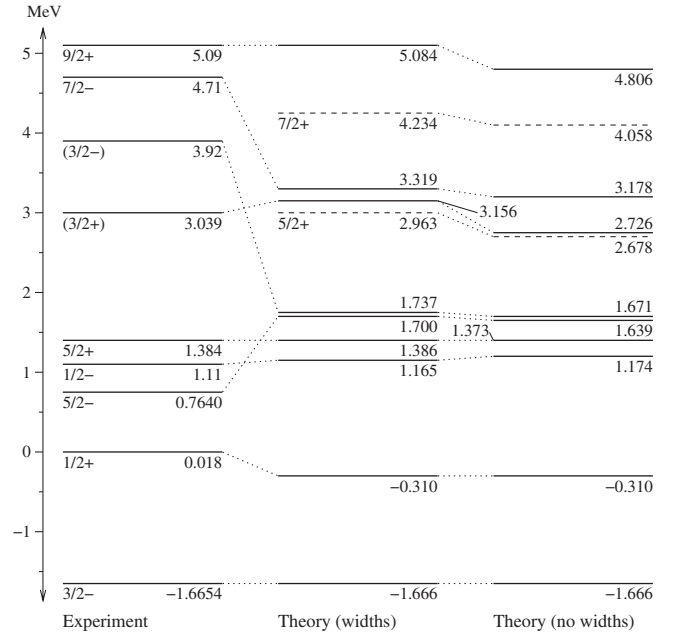
$J^\pi$	Centroid	(a)	(b)	(c)	(d)	(e)
$\frac{1}{2}^-$	-4.82	...	...	...	...	...
$\frac{1}{2}^+$	-2.04	...	...	...	...	...
$\frac{5}{2}^+$	-1.85	...	...	...	...	...
$\frac{3}{2}^-$	-1.36	...	...	...	...	...
$\frac{5}{2}^-$	0.16	$7 \times 10^{-10}$	0.09	0.18	0.28	0.37
$\frac{5}{2}^+$	1.95	0.01	0.10	0.19	0.28	0.38
$\frac{7}{2}^+$	2.62	$9 \times 10^{-7}$	0.09	0.18	0.28	0.37
$\frac{3}{2}^+$	2.74	0.04	0.13	0.23	0.33	0.42
$\frac{1}{2}^-$	2.75	$8 \times 10^{-4}$	0.27	0.55	0.82	1.11
$\frac{3}{2}^+$	3.25	0.45	0.50	0.56	0.61	0.67
$\frac{5}{2}^+$	4.06	0.13	0.25	0.38	0.52	0.66
$\frac{9}{2}^+$	4.51	$7 \times 10^{-4}$	0.09	0.19	0.28	0.38
$\frac{1}{2}^+$	4.76	0.52	0.71	0.92	1.14	1.37

has very little remnant of the compound system resonances. Clearly only the cross section from evaluation with three zero-width target states replicates measurement, but these evaluations are important, also, as they show that the target resonance method converges to the correct result in the limit.

Table II displays the widths of states in the compound nucleus,  $^{13}\text{C}$ , found using MCAS when attributing the diverse widths to the excited states of  $^{12}\text{C}$  listed in Table I. Note that, throughout this work, compound-system bound states were only calculated using target states of zero widths. The first column after  $J^\pi$  lists the bound state and resonance centroid energies obtained from the calculation made with the physically reasonable, zero-width excitation energies of the  $2_1^+$  and  $0_2^+$  states of  $^{12}\text{C}$ . Allowing those states to be resonances with the widths selected alters the state energy centroids by at most a few tens of keV, so these are not listed.

Thus, it is observed that allowing these target states to be resonances mostly affects widths of the resulting compound nucleus resonances. Those variations are consistent with changes noted in the cross section, with sharp resonances found for the zero-width state case rapidly disappearing and the others broadening to an extent that only a few are left distinguishable from a background. It is important to note, though, that all states in the compound system defined by the coupled-channel evaluations remain present, with, in this case, centroid energies little affected but widths increased.

The low excitation  $^8\text{Be}$  spectrum has a  $0^+$  ground state that has a small width for its decay into two  $\alpha$  particles ( $6 \times 10^{-6}$  MeV), a broad  $2^+$  resonance state with centroid at 3.03 MeV and width of 1.5 MeV, followed by a broader

FIG. 2. Experimental  $^9\text{Be}$  spectrum and that calculated from neutron scattering with stable and unstable  $^8\text{Be}$ .

$4^+$  resonance state with centroid at 11.35 MeV and width  $\sim 3.5$  MeV [9]. Two evaluations of the  $n + ^8\text{Be}$  cross section are obtained with MCAS; in both, the ground state is taken as having zero width. In the first, both the  $2^+$  and  $4^+$  states are also taken as zero width (ignoring their known  $\alpha$ -decay widths), whereas in the second, the widths evaluated from reaction data are used [9]. In both calculations, the same nuclear interaction is considered. It is taken from a rotor model with parameter values chosen in the finite-

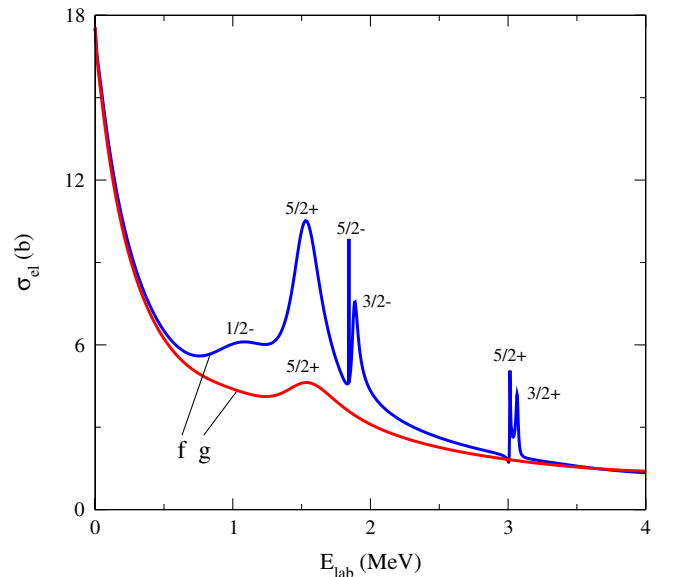
FIG. 3 (color online). Calculated cross sections for neutron scattering from (f) stable and (g) unstable  $^8\text{Be}$  as functions of neutron energy.

TABLE III.  ${}^9\text{Be}$  state centroids and widths ( $E$  and  $\Gamma$  in MeV) from calculation with  ${}^8\text{Be}$  states taken as zero width and then with known resonance widths, and experimental widths.

$J^\pi$	Zero width		Resonances		Experiment $\Gamma$ (exp.)
	$E(f)$	$\Gamma(f)$	$E(g)$	$\Gamma(g)$	
$\frac{3}{2}^-$	-1.67	...	...	...	...
$\frac{1}{2}^+$	-0.31	...	...	...	$0.217 \pm 0.001^a$
$\frac{1}{2}^-$	1.17	0.646	1.16	0.972	$1.080 \pm 0.110$
$\frac{5}{2}^+$	1.37	0.118	1.39	0.244	$0.282 \pm 0.011$
$\frac{5}{2}^-$	1.64	$3.7 \times 10^{-9}$	1.70	0.694	$7.8 \times 10^{-4}$
$\frac{3}{2}^-$	1.67	0.022	1.74	0.682	$1.330 \pm 0.360$
$\frac{5}{2}^+$	2.68	0.003	2.96	1.141	...
$\frac{3}{2}^+$	2.73	0.009	3.16	1.856	$0.743 \pm 0.055$
$\frac{7}{2}^-$	3.18	0.009	3.32	0.786	$1.210 \pm 0.230$
$\frac{7}{2}^+$	4.06	0.072	4.23	0.873	...
$\frac{9}{2}^+$	4.81	0.189	5.08	1.261	$1.330 \pm 0.090$

<sup>a</sup>This state is listed at 18 keV above threshold [9].

width states calculation to reproduce some aspects of the experimentally determined structure of  ${}^9\text{Be}$ , shown graphically in Fig. 2.

The results for the scattering cross sections are shown in Fig. 3. Upon introducing target state widths, as found in the  $n + {}^{12}\text{C}$  investigation, the resonances are suppressed but still present, their widths increasing and magnitudes decreasing so as all but the  $\frac{5}{2}^+$  cannot be discerned from the background. Compound system resonances of both calculations are at essentially the same energies. These effects are further illustrated by the centroid energies and widths of the resonances listed in Table III.

Column 1 of Table III (after  $J^\pi$ ) lists the resultant centroid energies of the spectrum found assuming the  $2_1^+$  and  $4_1^+$  excited states in  ${}^8\text{Be}$  have zero width, and the widths of these resonances (energies above the  $n + {}^8\text{Be}$  threshold) are in column 2. Columns 3 and 4 list energies and widths, respectively, obtained using the MCAS scheme on allowing the two excited states in  ${}^8\text{Be}$  to have their ascribed widths. Column 5 lists the experimental widths

[9]. As found in the study of the  ${}^{13}\text{C}$  spectrum, taking the excited states of  ${}^8\text{Be}$  to be resonances gives the same spectral list as when they are treated as zero width, but the widths of the compound nuclear states found significantly increase. This is again reflected in the cross sections. These increases bring the theoretical  ${}^9\text{Be}$  state widths closer, often significantly, to experimental values. In this case, some centroid energies are shifted by up to 330 keV.

In conclusion, a multichannel algebraic scattering approach to theoretical evaluation nucleon-nucleus scattering information has been extended to consider widths of target nucleus eigenstates. Resultant resonances in obtained cross sections suffer only minor changes to their energy centroids. However, their widths are substantially increased, often making them indistinguishable from the scattering background, but closer to experimentally determined widths. This was observed for  $n + {}^8\text{Be}$  scattering using calculations with and without experimental target state widths. Furthermore, it is found that this effect increases as target state widths increase, with sharp resonances quickly obscured.

This research was supported in part by Melbourne University PORES program. Travel support came also from Natural Sciences and Engineering Research Council, Canada, from INFN and Ministry of Research and Education, Italy (PRIN-project), the National Research Foundation (South Africa), and from the International Exchange program of the Australian Academy of Science.

\*pfraser@ph.unimelb.edu.au

- [1] K. Amos *et al.*, *Adv. Nucl. Phys.* **25**, 275 (2000).
- [2] A. Lagoyannis *et al.*, *Phys. Lett. B* **518**, 27 (2001).
- [3] S. V. Stepantsov *et al.*, *Phys. Lett. B* **542**, 35 (2002).
- [4] D. Ridikas *et al.*, *Nucl. Phys.* **A628**, 363 (1998).
- [5] K. Amos *et al.*, *Nucl. Phys.* **A728**, 65 (2003).
- [6] S. Weinberg, in *Lectures on Particles and Field Theory*, Brandeis Summer Institute in Theoretical Physics Vol. 2 (Prentice-Hall, Englewood Cliffs, NJ, 1965), p. 289.
- [7] L. Canton *et al.*, *Phys. Rev. Lett.* **94**, 122503 (2005).
- [8] K. Amos *et al.*, *Phys. Rev. C* **72**, 064604 (2005).
- [9] D. R. Tilley *et al.*, *Nucl. Phys.* **A745**, 155 (2004).